frontiers | Frontiers in Materials

TYPE Original Research
PUBLISHED 12 April 2023
DOI 10.3389/fmats.2023.1125462

OPEN ACCESS

EDITED BY
Liming Dai,
Case Western Reserve University,
United States

REVIEWED BY
Dong Ryeol Whang,
Hannam University, Republic of Korea
Fujun Tao,
Argonne National Laboratory (DOE),
United States

*CORRESPONDENCE
Turan Ozturk,
ozturktur@itu.edu.tr
Ceylan Zafer,
ceylan.zafer@ege.edu.tr

SPECIALTY SECTION
This article was submitted
to Energy Materials,
a section of the journal
Frontiers in Materials

RECEIVED 16 December 2022
ACCEPTED 29 March 2023
PUBLISHED 12 April 2023

CITATION
Isci R, Unal M, Yesil T, Ekici A, Sütay B, Zafer C and Ozturk T (2023), Thieno[3,2-*b*]thiophene and triphenylamine-based hole transport materials for perovskite solar cells.
Front. Mater. 10:1125462.
doi: 10.3389/fmats.2023.1125462

Thieno[3,2-*b*]thiophene and triphenylamine-based hole transport materials for perovskite solar cells

Recep Isci[1], Melis Unal[1], Tamer Yesil[2], Alper Ekici[2], Berkay Sütay[1], Ceylan Zafer[2]* and Turan Ozturk[1,3]*

[1]Chemistry Department, Istanbul Technical University, Istanbul, Türkiye, [2]Institute of Solar Energy, Ege University, Izmir, Türkiye, [3]Chemistry Group Laboratories, TUBITAK UME, Kocaeli, Türkiye

Heterocyclic compounds have played significant roles in achieving high performance as hole transport materials (HTMs) for perovskite solar cell (PSC) applications. Various studies have focused on the development of fused heterocyclic conjugated structures for hole transport materials. In this report, three novel π-extended conjugated materials (M1-M3), based on thieno[3,2-*b*]thiophene (TT) and 4,4′-dimethoxytriphenylamine [TPA(OMe)$_2$], were designed and successfully synthesized *via* Palladium (0) catalyzed Suzuki coupling reaction. Their optical, electrochemical, and thermal properties were investigated by UV-Vis, fluorescence, cyclic voltammetry, and thermal analysis. The materials were utilized as hole transport materials in p-i-n architecture perovskite solar cells, which displayed performances of open-circuit voltage (V_{oc}) as high as 1,050 mV, a maximum short-circuit current (J_{sc}) of 16,9 mA/cm^2, a maximum fill factor (FF) of 29.3%, and a power conversion efficiency (PCE) of 5.20%. This work demonstrated that thieno[3,2-*b*]thiophene and TPA(OMe)$_2$-based structures are promising cores for high-performance hole transport materials in perovskite solar cell architecture.

KEYWORDS

thieno[3,2-b]thiophene, triphenylamine, hole transport materials, solution processable, perovskite solar cell

1 Introduction

Organic perovskites have received significant attention over the past two decades due to the utility of solar energy (Peak et al., 2016; Liu et al., 2017; Zhang et al., 2017). Regarding their performances, perovskite solar cells (PSCs) highly depend on hole-transporting materials (HTMs), which play a crucial role in hole extracting and transferring (Lv et al., 2015; Wu et al., 2018; Sharma et al., 2021). As a general approach, current is generated in PSCs through the flow of photogenerated electrons (e^-) from the perovskite layer to the electron transport layer (ETL) and holes (h^+), and to the hole transport layer (HTL) (Xu et al., 2020; Afanasyev et al., 2021).

Organic hole conductors essentially include two categories: (i) small molecular and (ii) polymeric materials (Turksoy et al., 2003; Ertas et al., 2004; Akman et al., 2020; Chen et al., 2021; Farokhi et al., 2022). Small molecular HTMs have some advantages over polymers such as defined molecular structure, definite molecular weight, easy purification, and good batch-to-batch reproducibility (Lin et al., 2020; Pan et al., 2020; Tavasli et al., 2022; Yildiz et al.,

2017; M'Baye et al., 2007). Among them, TAA-based compounds are the most widely used HTMs in PSCs due to their excellent charge transport capabilities (Isci et al., 2020a; Isci, 2020b; Isci, 2021a; Isci, 2022a). Furthermore, the presence of phenylamines in the molecular structure of organic polymers confers unique mechanical features (Wang et al., 2016; Isci et al., 2022b; Farokhi et al., 2022; Quezada-Borja et al., 2022). Thienothiophenes have been attractive small, conjugated compounds for synthesizing semiconducting polymers and are widely used as building blocks for organic materials as they have electron-rich, flat, rigid, and good electron delocalized skeleton, prolonged molecular conjugation, intermolecular S. . .S interactions, and chemical stability (Ozturk et al., 1995; Saygili et al., 2001; Osken et al., 2012; Cinar et al., 2015; Isci et al., 2021b; 2022d). Thieno[3,2-*b*] thiophene, in particular, is the most conjugated and stable isomer of TTs, having interesting electronic and optical properties. It has been examined and used in various energy-based organic electronic applications by our group such as OLED (Isci et al., 2020a; 2022a), OFET (Amna et al., 2022), electrocatalyst (Isci et al., 2022d), capacitor (Topal et al., 2021), and memory (Gunturkun et al., 2022).

In this study, we report the synthesis and characterization of three novel 4,4′-dimethoxytriphenylamine [TPA(OMe)$_2$] and thieno[3,2-*b*]thiophene (TT)-based conjugated materials, having different electronic substituents such as C_6H_{13}, 4-PhOMe, and Ph. Their photophysical and electrochemical properties were investigated by UV-Vis spectroscopy, emission spectroscopy, and cyclic voltammetry. Moreover, they were used as small molecules in hole transport materials (HTMs). M1-M3 displayed remarkable properties such as mega Stokes shift of 5,067 cm^{-1}, optic band gaps changing between 2.80 and 2.67 eV, and theoretical band gaps around 2.35 eV, which are consistent with the experimental results. The maximum fill factor reached 32.4% and the maximum Voc was measured to be 1,050 mV in device fabrications. This work demonstrated that the introduction of a TT core is a promising strategy for achieving high performance of HTMs toward PSCs.

2 Materials and methods

All the reagents purchased from Sigma-Aldrich and Acros Organics were used without further purification, and the solvents used in the syntheses were of technical grade. Column chromatography was performed with ≤0.063 μm silica gel for purification. ^{1}H and ^{13}C NMR spectra were recorded on Varian 500 and 126 MHz spectrometers, respectively. Proton and carbon chemical shifts were reported in parts per million downfield from tetramethylsilane (TMS). FTO glasses, cut in 2.5 cm^2 × 2.5 cm^2 (OPV-FTO22-15, 14Ω/□), were purchased from OPV Tech. Hydrochloric acid (37%), 4-tert-butylpyridine (TBP, 98.0%), isopropyl alcohol (HPLC Grade, 99.9%), acetonitrile (ACN, technical grade, 99.8%), chlorobenzene (anhydrous, 99.8%), titanium isopropoxide {Ti[OCH(CH_3)$_2$]$_4$, 97%}, and cesium iodide (CsI, 99.999%) were acquired from Merck. Lead iodide (PbI_2, 99.99%) was purchased from Tokyo Chemical Industries. Methylammonium bromide (MABr, >99.5%), lead bromide ($PbBr_2$ 99.999%), and formamidinium iodide (FAI, >99.5%) were obtained from Lumtec. Bis(trifluoromethane)sulfonimide lithium salt (Li-TFSI, 99.0%) and DMF (anhydrous, >99.5%) were purchased from Acros Organics. DMSO (>99.7) and Spiro-OMeTAD {2,2′,7,7′-tetrakis[N,N-di(4-methoxyphenyl) amino]-9,9′-spirobifluorene} were bought from Merck and Borun New Material Technology, respectively.

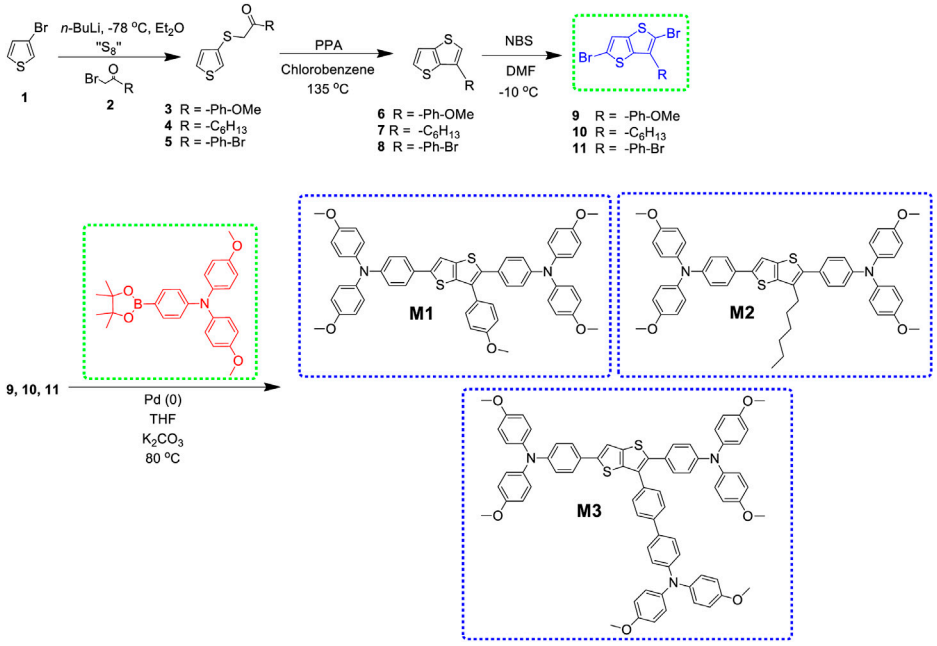

SCHEME 1
Synthetic route of the materials M1-M3.

TABLE 1 Optical and electronic data of M1-M3.

Molecules	UV_{max}[a] (nm)	UV_{onset} (nm)	UV_{max}[b] (nm)	Fl_{max}[a] (nm)	Stokes shift (nm)	$\Delta\nu$[c] (cm^{-1})	E_{optic}[d] (eV)	E_{ons}[e] (V)	HOMO[f] (V)	LUMO[g] (V)
M1	401	458	429	492	91	4,612	2.71	0.65	−5.05	−2.34
M2	389	445	394	477	88	4,742	2.80	0.68	−5.08	−2.28
M3	404	464	468	508	104	5,067	2.67	0.61	−5.01	−2.34

[a]Absorption and emission maxima in THF.
[b]Absorption maxima on ITO.
[c]$\Delta\nu = 1/\lambda_{abs,\ max} - 1/\lambda_{emission}$.
[d]E_{opt} from the onset of absorption spectra in THF.
[e]Oxidation onset potential from CV.
[f]HOMO = −(4.40 + $E_{(onset)ox}$) eV.
[g]LUMO = (HOMO + E_{optic}) eV.

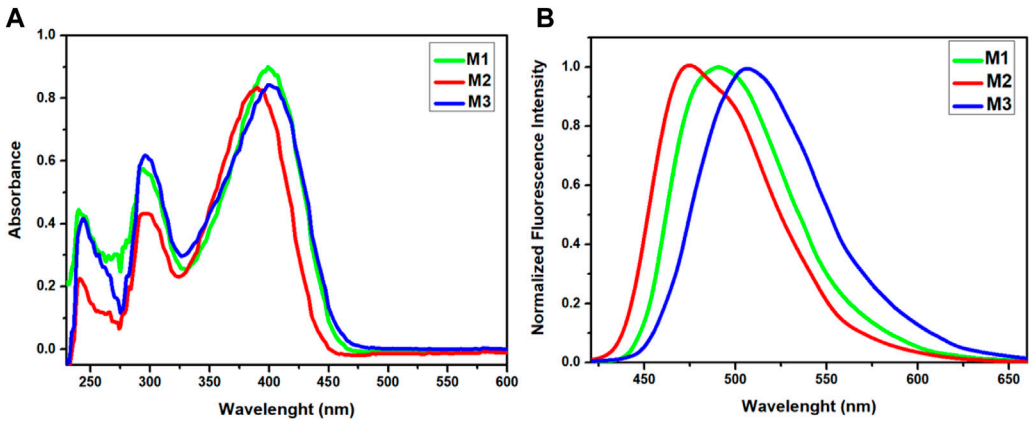

FIGURE 1
(A) UV-vis absorption spectra and **(B)** emission spectra of M1-M3 in THF.

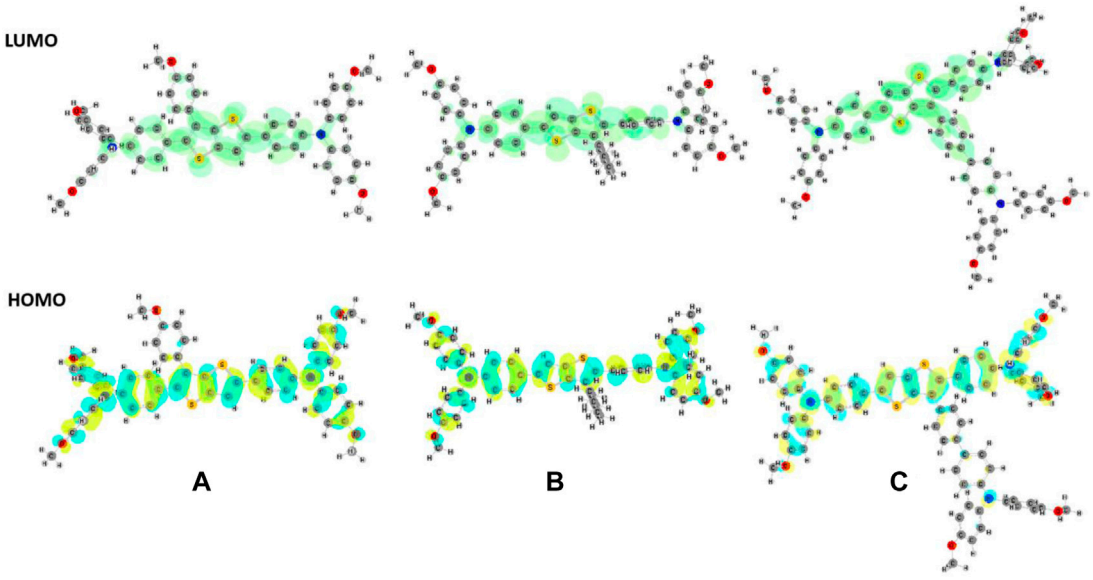

FIGURE 2
Optimized geometries (in THF) and HOMO (below) and LUMO (above) frontier orbitals of **(A)** M1, **(B)** M2, and **(C)** M3 molecules.

TABLE 2 The calculated energies of the frontier orbitals, HOMO-LUMO energy gap (Δ), λ_{max}, λ_{onset}, and optical band gap values (in THF) for the studied molecules.

Molecules	HOMO (eV)	LUMO (eV)	Δ (eV)	λ_{max} (nm)	λ_{onset} (nm)	E_{optic} (eV)
M1	−4.88	−1.36	3.52	424	516	2.40
M2	−4.88	−1.41	3.47	431	527	2.35
M3	−4.89	−1.45	3.44	434	532	2.33

TABLE 3 HTM performances of M1-M3.

Materials	J_{SC} (mA.cm^{-2})	Voc (mV)	FF (%)	PCE (%)
M1	12.4	980	32.4	3.94
M2	4.53	630	25.5	0.73
M3	16.9	1,050	29.3	5.20
Spiro-OMeTAD	19.5	870	42.0	7.14

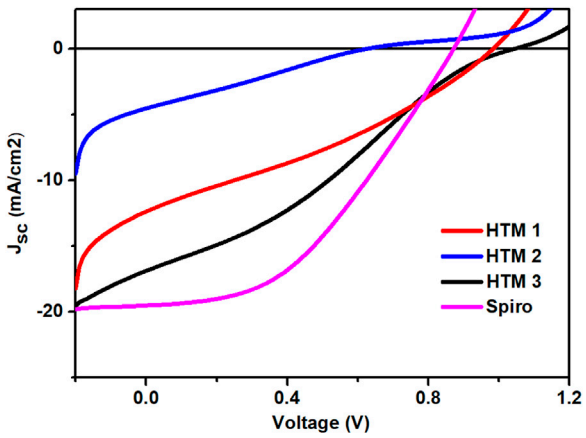

FIGURE 3
Current (J)–voltage (V) curves of the solar cells with HTM 1-3 (M1-M3) and Spiro-OMeTAD.

3 Result and discussion

3.1 Design and synthesis

The monoketones (3-5), TTs (6-8), some of the dibrominated TTs (9, 11), and 4,4′-dimethoxytriphenylamine [TPA(OMe)$_2$] were synthesized following our previous reports (Isci et al., 2020a; Isci, 2021a). Initially, the synthesis of the core units, thieno[3,2-*b*] thiophenes 3-5, was conducted starting from 3-bromothiophene (1). The monoketones, 3-5, were constructed in a one-pot three-step reaction: (i) lithiation of 3-bromothiophene (1) with *n*-butyllithium at −78°C, (ii) additions of elemental sulfur, and then (iii) α-haloketones. The yields were calculated to be 55%, 90%, and 85%, respectively. Their ring closure reactions were conducted in the presence of polyphosphoric acid (PPA) in refluxing chlorobenzene to give 6-8 in 87%, 85%, and 80% yields, respectively. The dibrominated TTs 9-11 were obtained through selective dibromination of 6-8 using NBS at −10°C in DMF in 85%, 80%, and 90% yields, respectively. Their Suzuki coupling reactions with boronated 4,4′-dimethoxytriphenylamine produced the target functionalized thienothiophenes M1-M3 in 55%, 60%, and 65% yields, respectively (Scheme 1).

3.2 Optical properties

Photophysical properties (UV-Vis absorption and emission spectra) of the compounds were investigated in THF at room temperature (Table 1; Figure 1A). The maximum π-π* absorption wavelengths (λ_{max}) of the compounds M1-M3 were measured to be 401, 389, and 404 nm, respectively. The absorbances of the TTs showed increasing bathochromic shift from hexyl (-C_6H_{13}) to dimethoxytriphenylamine para substituents, indicating that high electron donating dimethoxytriphenylamine substituted M3 exhibited the higher bathochromic shifts of π-π* transitions, compared to weak electron-donating hexyl (-C_6H_{13})-substituted M2. M1, having 4-MeOPh, which is a weaker electron donor than dimethoxytriphenylamine but a stronger donor than hexyl, had absorbance between M2 and M3. From the absorption spectra, the onset maximums of 458, 445, and 464 nm were observed for M1-M3, respectively. Then, the optical band gaps of the polymers were determined to be 2.71 (M1), 2.80 (M2), and 2.66 eV (M3).

The fluorescence measurements of the materials were performed in THF (Table 1; Figure 1B). They displayed emission maxima of 492 (M1), 477 (M2), and 508 nm (M3). A similar trend, i.e., the longest emission with M3 (540 nm), was observed, which could be due to the presence of more electron-donating units compared to the others, providing the system with a more efficient charge-transfer property. The Stokes shifts ranged from 88 (M2) to 104 (M3) nm. Mega Stokes shift (>100 nm) of M3 indicated a fast relaxation from the excited state to the ground state owing to intramolecular charge transfer between TT and 4,4′-dimethoxytriphenylamine groups.

In addition to the measurements in solution, absorption properties of the materials spin-coated on ITO were investigated. Solid-state UV maximums were measured to be 429 (M1), 394 (M2), and 468 nm (M3) (Supplementary Figure S1; Table 1). As expected, solid-state absorptions had red shifts compared to their absorptions in THF, signifying an enhancement of π-conjugation and good π-stacking in their film forms.

3.3 Electrochemical properties

Regarding potential applications of the materials as organic electronics, their electrochemical properties have significant as

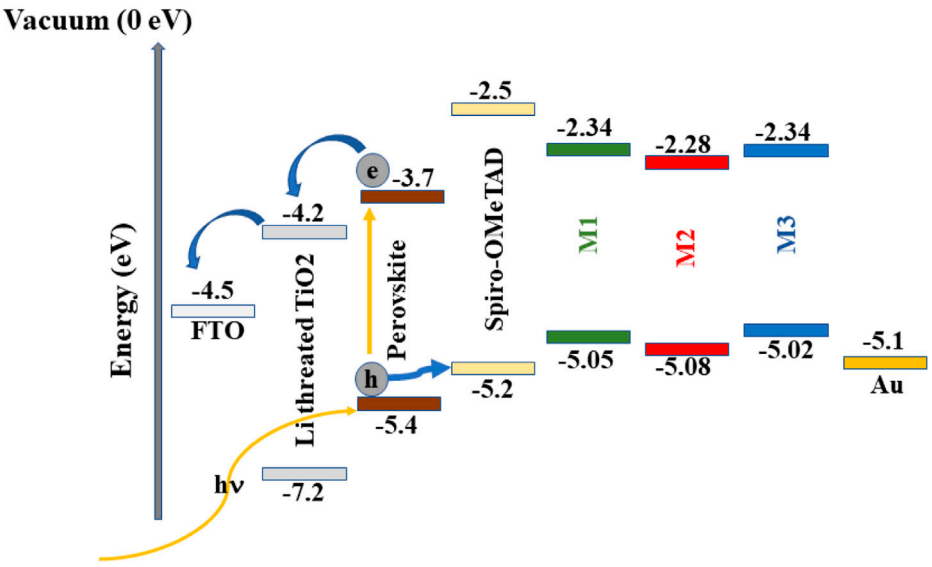

FIGURE 4
The energy level diagram of PSC.

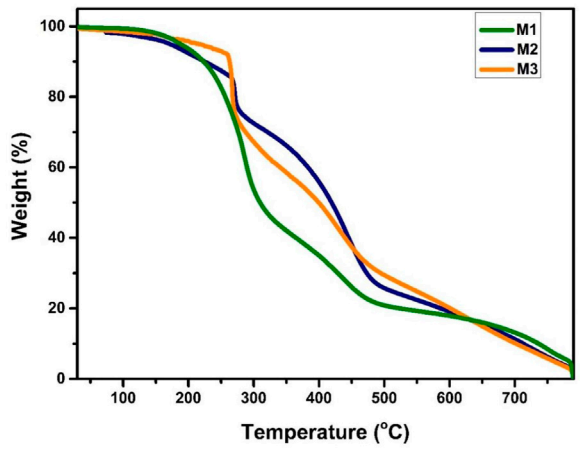

FIGURE 5
TGA diagram of the materials M1-M3.

well as optical features. The HOMO and LUMO levels play important roles in charge injection and charge transport of active materials in device fabrications. The electrochemical features were conducted by cyclic voltammetry (CV) measurement in a mixture of dichloromethane/acetonitrile (1: 1) in the presence of tetrabutylammonium hexafluorophosphate ($TBAPF_6$) as an electrolyte at a scan rate of 100 $mV{\cdot}s^{-1}$, using Pt wires as counter and working electrodes and Ag wire as a reference electrode (Supplementary Figure S2). The oxidation onset potentials (E_{onset}) were observed to be 0.65, 0.68, and −0.61 V for M1-M3, respectively. On the basis of the oxidation onset potentials and optical band gaps, the HOMO/LUMO energies of the materials were calculated to be −5.05/−2.34, −5.08/−2.28, and −5.01/−2.34 eV, respectively, using the equations of HOMO = $-(E_{onset} + 4.40)$ (eV) and LUMO = (HOMO + E_{optic}) eV (Table 1). With the highest HOMO energy level, M3 with three $TPA(OMe)_2$ substituents confirmed the presence of the best electron-donating moieties. A higher HOMO level presents increased donor ability. While M2 with weak electron-donating alkyl substituent had the lowest HOMO level, M1 remained between M2 and M3. The results were in good agreement with both theoretically predicted energy gaps and experimental optic band gaps (Table 1).

3.4 Computational chemistry

The structures of the molecules were modeled by using density functional theory (DFT). Geometry optimizations were conducted at B3LYP/6-31G (d, p) level of theory in the implicit THF medium ($\varepsilon = 7.4257$), applying conductor-like polarizable continuum solvent model (CPCM) (Cossi et al., 2003). All computations were performed using the Gaussian'16 program package (Frisch et al., 2016). The optimized geometries and the related frontier orbitals are given in Figure 2.

The HOMO orbital was found to be delocalized over the main skeleton of the molecule, while the LUMO orbital was mainly located on the TT unit and the adjacent rings. Time-dependent DFT (TD-DFT) calculations were performed at the PBE0 level of theory in the same basis set in solvent media to compute the theoretical band gaps and characteristic wavelengths. The optical band gaps were predicted and calculated from the λ_{onset} of the UV curves (Table 2). Theoretically predicted optical band gaps were found to be consistent with the corresponding experimental data.

3.5 Device fabrications

J-V curves were obtained using a solar simulator equipped with a Keithley 2400 source meter without any prior conditioning. A light source with an AM1.5G filter was used, and 100 mW/cm^2 intensity of light was maintained during all J-V measurements. Before each measurement, the light power was confirmed using a calibrated silicon reference solar cell with a 4 cm^2 area. The voltage scan was realized with a fixed rate of 10 $mV{\cdot}s^{-1}$ for collecting photovoltaic parameters, and the voltage sweep was set to start from negative to positive during all J-V measurements. The average photovoltaic parameters for the cells were calculated from data collected from four devices for each batch of materials. J_{sc} values were measured as 12.4, 4.53, and 16.9 $mA{\cdot}cm^{-2}$ for M1-M3, respectively. The higher J_{sc} value of M3 compared to other HTMs was attributed to a better intramolecular charge transfer between TT and 4,4′-dimethoxytriphenylamine moieties. Considering that M3 had a better intramolecular charge transfer, it was expected to collect photo-induced free charge carriers generated in the perovskite layer more efficiently than M1 and M2 with minimum recombination losses through metal contacts.

Methoxy (-OCH_3) functional groups on the HTMs are responsible for the molecular arrangement as well as intermolecular charge transfer *via* alignment of the HOMO energy level of the HTM molecules. Although the methoxy group has an electron-withdrawing inductive effect, it can also exhibit electron-donating behaviors depending on the substitution of ortho, para, and meta positions to the phenyl functional group under resonance stabilization which is called the mesomeric effect (Jeon et al., 2014). V_{oc} values were measured as 980, 630, and 1,050 mV for M1, M2, and M3, respectively, which were found to be consistent with J_{sc} and PCE values, indicating that charge recombination ratios at the perovskite/HTM interface are lower with M3. The recombination rate is strongly effective on the J_{sc} values as well as V_{oc} and FF. Parallel resistance (Rp) is much larger in the case where M3 HTM is used compared to M1 and M2, where the recombination ratio is minimized (Figures 3, 4). Attributing the Voc directly to the difference in HOMO energy levels of the HTMs is thought to be misleading as the distinction between both experimental and calculated HOMO energy levels of the molecules are very close to each other.

Functionalizing the main core of TT with methoxybenzene and 4,4′-dimethoxytriphenylamine moieties was found to be a promising strategy for adjusting HOMO energy levels to be compatible with the HOMO energy level of the perovskite material for extracting holes efficiently (Wu et al., 2018). Also, high LUMO energy levels of HTMs can efficiently act as an electron blocker and prevent short-circuit. Finally, this molecular design strategy is found to be promising for obtaining high J_{sc} values due to better intramolecular charge transfer.

The current-voltage curves of the devices, fabricated with the given novel hole transport materials, exhibited relatively low fill factors of 32.4%, 25.5%, and 29.3% for M1-M3, respectively, which could be due to high levels of series resistance. This is known to occur with first and higher orders of recombination. The first order of recombination, being surface type and trap-assisted recombinations, is thought to be the primary reason for the relatively low fill factor, given the fact of apparent morphological inconsistencies on the surface of the coated HTM (Wolff et al., 2021). Low parallel resistance is also evident, as it is thought to be due to the defects in the interface of the p-n junction, where the charges are ineffectively separated, which is the interface between the absorber perovskite and the HTM. This causes local short circuits within the device.

As a result of relatively good J_{sc} and V_{oc} values, PCE values of 3.94, 0.73, and 5.2, corresponding to M1-M3 were obtained, respectively (Table 3). Comparable device parameters indicate that these novel HTMs can pave the way for forthcoming TT-based molecules as promising candidates for a typical perovskite solar cell architecture.

3.6 Thermal properties

The thermal properties of the M1-M3 were investigated by thermal gravimetric analysis (TGA) at 800°C at a heating rate of 10°C min^{-1} under an N_2 atmosphere. Although all materials showed high thermal stability with similar degradation profiles, different para substituents on the TT cores led to different thermal behaviors. While the first decomposition temperatures (Td, corresponding to 5% weight loss) of M1 and M2 were measured to be at around 185°C and 167°C, respectively, M3 had a decomposition temperature of 261°C (Figure 5). M3 had relatively better thermal stability compared to M1 and M2, indicating that -$TPA(OMe)_2$ substituent on the M3 skeleton provided higher thermal resistance, possibly, due to having more aromatic units compared to -PhOMe and -C_6H_{13} functional groups on M2 and M3, respectively.

4 Conclusion

In summary, three novel thienothiophene (TT) and 4,4′-dimethoxytriphenylamine [TPA(OMe)2]-based conjugated molecules (M1-M3) were successfully synthesized using the Suzuki coupling method. Their photophysical and electrochemical properties were investigated both experimentally and theoretically. M1-M3 were applied as hole transporting materials (HTMs), reaching overall conversion efficiency of 5.2% in p-i-n architecture perovskite solar cells. Additionally, molecular structures, electronic HOMO–LUMO levels, optic band gaps, and device performances were compared with each other. Moreover, experimental optoelectronic analyses were supported by theoretical studies based on density functional theory (DFT) calculations. This study offers a facile approach for developing new HTMs that could boost the PSC performance *via* molecular engineering using thienothiophene and triphenylamine units (Topal et al., 2022, Isci et al., 2022c).

Data availability statement

The original contributions presented in the study are included in the article/Supplementary Material, further inquiries can be directed to the corresponding authors.

Author contributions

RI: writing-original draft, methodology, formal analysis, and investigation. MU, TY, and AE: investigation, methodology, and data curation. BS: formal analysis and software. CZ and TO: project conceptualization, supervision, and editing. All authors have read and approved the manuscript for publication.

Funding

We thank the Higher Education Council of Türkiye (YOK) and TUBITAK grants to RI (PhD., 100/2000 YOK and 2211A BIDEP/TUBITAK); ITU (Istanbul Technical University), 122Z568 numbered TUBITAK 1001 Project; TY within the Program nr: 2211/C (Grant nr: 1649B032100473); and Unsped Global Lojistik, Türkiye, for the financial support. The computing resources used in this work were provided by the National Center for High-Performance Computing (UHeM) under grant number 1010722021.

Conflict of interest

The authors declare that the research was conducted in the absence of any commercial or financial relationships that could be construed as a potential conflict of interest.

Publisher's note

All claims expressed in this article are solely those of the authors and do not necessarily represent those of their affiliated organizations, or those of the publisher, the editors and the reviewers. Any product that may be evaluated in this article, or claim that may be made by its manufacturer, is not guaranteed or endorsed by the publisher.

Supplementary material

The Supplementary Material for this article can be found online at: https://www.frontiersin.org/articles/10.3389/fmats.2023.1125462/full#supplementary-material

References

Afanasyev, D., Ibrayev, N., and Nuraje, N. (2021). Effect of plasmonic nanostructures on the optical properties of CH_3NH_3PbI perovskite films. *Front. Mat.* 7, 600424. doi:10.3389/fmats.2020.600424

Akman, E., Akin, S., Ozturk, T., Gulveren, B., and Sonmezoglu, S. (2020). Europium and terbium lanthanide ions co-doping in TiO2 photoanode to synchronously improve light-harvesting and open-circuit voltage for high-efficiency dye-sensitized solar cells. *Sol. Energy* 202, 227–237. doi:10.1016/j.solener.2020.03.108

Amna, B., Isci, R., Siddiqi, H. M., Majewski, L. A., Faraji, S., and Ozturk, T. (2022). High performance, low-voltage organic field-effect transistors using thieno[3,2-*b*]thiophene and benzothiadiazole Co-polymers. *J. Mat. Chem. C* 10 (21), 8254–8265. doi:10.1039/d2tc01222g

Chen, Z., He, P., Wu, D., Chen, C., Mujahid, M., Li, Y., et al. (2021). Processing and preparation method for high-quality opto-electronic perovskite film. *Front. Mat.* 8, 723169. doi:10.3389/fmats.2021.723169

Cinar, M. E., and Ozturk, T. (2015). Thienothiophenes, dithienothiophenes, and thienoacenes: Syntheses, oligomers, polymers, and properties. *Chem. Rev.* 115 (9), 3036–3140. doi:10.1021/cr500271a

Cossi, M., Rega, N., Scalmani, G., and Barone, V. (2003). Energies, structures, and electronic properties of molecules in solution with the C-PCM solvation model. *J. Comput. Chem.* 24 (6), 669–681. doi:10.1002/jcc.10189

Ertas, E., and Ozturk, T. (2004). A new reaction of P_4S_{10} and lawesson's reagent; a new method for the synthesis of dithieno[3,2-b;2′,3′-d]thiophenes. *Tetrahedron Lett.* 45 (17), 3405–3407. doi:10.1016/j.tetlet.2004.03.023

Farokhi, A., Shahroosvand, H., Monache, G. D., Melanie Pilkington, M., and Nazeeruddin, M. K. (2022). The evolution of triphenylamine hole transport materials for efficient perovskite solar cells. *Chem. Soc. Rev.* 51, 5974–6064. doi:10.1039/d1cs01157j

Frisch, M. J., Trucks, G. W., Schlegel, H. B., Scuseria, G. E., Robb, M. A., and Cheeseman, J. R. (2016). *Gaussian 16, revision C.01*. Wallingford CT: Gaussian, Inc.

Gunturkun, D., Isci, R., Sütay, B., Majewski, L. A., Faraji, S., and Ozturk, T. (2022). Copolymers of 3-Arylthieno[3,2-*b*]thiophenes bearing different substituents: Synthesis, electronic, optical, sensor and memory properties. *Eur. Polym. J.* 170, 111167. doi:10.1016/j.eurpolymj.2022.111167

Isci, R., Balkan, T., Tafazoli, S., Sütay, B., Eroglu, M. S., and Ozturk, T. (2022d). Thienothiophene and triphenylbenzene based electroactive conjugated porous polymer for oxygen reduction reaction (ORR). *ACS Appl. Energy Mat.* 5 (11), 13284–13292. doi:10.1021/acsaem.2c01830

Isci, R., Baysak, E., Kesan, G., Minofar, B., Eroglu, M. S., Duygulu, O., et al. (2022c). Noncovalent modification of single wall carbon nanotubes (SWCNTs) by thienothiophene derivatives. *Nanoscale* 14, 16602–16610. doi:10.1039/D2NR04582F

Isci, R., Gunturkun, D., Yalin, A. S., and Ozturk, T. (2021b). Copolymers of 4-thieno[3,2-*b*]thiophen-3-ylbenzonitrile with anthracene and biphenyl; synthesis, characterization, electronic, optical, and thermal properties. *J. Polym. Sci.* 59 (1), 117–123. doi:10.1002/pol.20200635

Isci, R., Tekin, E., Kaya, K., Mucur, P. S., Gorkem, S. F., and Ozturk, T. (2020a). Tetraphenylethylene substituted thienothiophene and dithienothiophene derivatives: Synthesis, optical properties and OLED applications. *J. Mat. Chem. C* 8, 7908–7915. doi:10.1039/D0TC01715A

Isci, R., Tekin, E., Mucur, S. P., and Ozturk, T. (2020b). A bifunctional bulky thienothiophene derivative; synthesis, electronic-optical properties and OLED applications. *ChemistrySelect* 5 (42), 13091–13098. doi:10.1002/slct.202003273

Isci, R., Unal, M., Kucukcakir, G., Gurbuz, N. A., Gorkem, S. F., and Ozturk, T. (2021a). Triphenylamine/4,4′-Dimethoxytriphenylamine-Functionalized thieno[3,2-*b*]thiophene fluorophores with a high quantum efficiency: Synthesis and photophysical properties. *J. Phys. Chem. B* 125 (48), 13309–13319. doi:10.1021/acs.jpcb.1c09448

Isci, R., Varzeghani, A. R., Kaya, K., Sütay, B., Tekin, E., and Ozturk, T. (2022a). Triphenylamine/tetraphenylethylene substituted 4-Thieno[3,2-*b*]thiophen-3-ylbenzonitriles: Synthesis, photophysical-electronic properties, and applications. *ACS Sustain. Chem. Eng.* 10 (4), 1605–1615. doi:10.1021/acssuschemeng.1c07240

Isci, R., Wan, L., Topal, S., Gunturkun, D., Campbell, A. J., and Ozturk, T. (2022b). Solution-processable donor-π-acceptor type thieno[3,2-*b*]Thiophene derivatives; synthesis, photophysical properties and applications. *J. Mat. Chem. C* 10 (29), 10719–10727. doi:10.1039/d2tc02371g

Jeon, N. J., Lee, H. G., Kim, Y. C., Seo, J., Noh, J. H., Lee, J., et al. (2014). o-Methoxy substituents in spiro-OMeTAD for efficient inorganic–organic hybrid perovskite solar cells. *J. Am. Chem. Soc.* 136 (22), 7837–7840. doi:10.1021/ja502824c

Lin, C. (2020). Stabilizing organic-inorganic lead halide perovskite solar cells with efficiency beyond 20. *Front. Chem.* 8, 592. doi:10.3389/fchem.2020.00592

Liu, X., Kong, F., Guo, F., Cheng, T., Chen, W., Yu, T., et al. (2017). Influence of π-linker on triphenylamine-based hole transporting materials in perovskite solar cells. *Dyes Pigm* 139, 129–135. doi:10.1016/j.dyepig.2016.12.022

Lv, S., Song, Y., Xiao, J., Zhu, L., Shi, J., Wei, H., et al. (2015). Simple triphenylamine-based hole-transporting materials for perovskite solar cells. *Electrochim. Acta.* 182, 733–741. doi:10.1016/j.electacta.2015.09.165

M'Baye, G., Klymchenko, A. S., Yushchenko, D. A., Shvadchak, V. V., Ozturk, T., Mély, Y., et al. (2007). Fluorescent dyes undergoing intramolecular proton transfer with improved sensitivity to surface charge in lipid bilayers. *Photochem. Photobiol. Sci.* 6 (1), 71–76. doi:10.1039/B611699J

Osken, I., Sahin, O., Gundogan, A. S., Bildirir, H., Capan, A., Ertas, E., et al. (2012). Selective syntheses of vinylenedithiathiophenes (VDTTs) and dithieno[2,3-*b*;2′,3′-*d*]thiophenes (DTTs); building blocks for π-conjugated systems. *Tetrahedron* 68 (4), 1216–1222. doi:10.1016/j.tet.2011.11.059

Ozturk, T., Rice, C. R., and Wallis, J. D. (1995). Synthesis of a chiral monosubstituted derivative of bis(ethylenedithio)tetrathiafulvalene: Reaction of the cyclic sulfate ester of

R,R-1,4-difluorobutane-2,3-diol with 2-thioxo-1,3-dithiole-4,5-dithiolate. *Mat. Chem.* 5, 1553–1556. doi:10.1039/JM9950501553

Paek, S., Zimmermann, I., Gao, P., Gratia, P., Rakstys, K., Grancini, G., et al. (2016). Donor–π–donor type hole transporting materials: Marked π-bridge effects on optoelectronic properties, solid-state structure, and perovskite solar cell efficiency. *Chem. Sci.* 7 (9), 6068–6075. doi:10.1039/C6SC01478J

Pan, X., Sharma, A., Kroon, R., Gedefaw, D., Elmas, S., Yin, Y., et al. (2020). Water/ethanol soluble p-type conjugated polymers for the use in organic photovoltaics. *Front. Mat.* 7, 281. doi:10.3389/fmats.2020.00281

Quezada-Borja, J. D., Rodríguez-Valdez, L. M., Palomares-Báez, J. P., Chávez-Rojo, M. A., Landeros-Martinez, L. -L., Martínez-Ceniceros, M. C., et al. (2022). Design of new hole transport materials based on triphenylamine derivatives using different π-linkers for the application in perovskite solar cells. A theoretical study. *Front. Chem.* 10, 907556. doi:10.3389/fchem.2022.907556

Saygili, N., Brown, R. J., Day, P., Hoelzl, R., Kathirgamanathan, P., Mageean, E. R., et al. (2001). Functionalised organosulfur donor molecules: Synthesis of racemic hydroxymethyl-alkoxymethyl- and dialkoxymethyl-bis(ethylenedithio) tetrathiafulvalenes. *Tetrahedron* 57 (23), 5015–5026. doi:10.1016/S0040-4020(01)00432-X

Sharma, A., Singh, S., Song, X., Rosas Villalva, D., Troughton, J., Corzo, D., et al. (2021). A nonionic alcohol soluble polymer cathode interlayer enables efficient organic and perovskite solar cells. *Chem. Mater.* 33, 8602–8611. doi:10.1021/acs.chemmater.1c01430

Tavasli, A., Gurunlu, B., Gunturkun, D., Isci, R., and Faraji, S. (2022). A review on solution-processed organic phototransistors and their recent developments. *Electronics* 11 (3), 316. doi:10.3390/electronics11030316

Topal, S., Isci, R., Sezer, E., Ozturk, T., and Ustamehmetoglu, B. (2021). Synthesis and electropolymerization of 3-arylthieno[3,2-*b*]thiophenes and triphenylamine based comonomers. *Electrochim. Acta.* 389, 138688. doi:10.1016/j.electacta.2021.138688

Topal, S., Isci, R., Topal, S., Karakaya, O., Amna, B., Gunturkun, D., et al. (2022). 1,3-Dithioles. *CHEC IV* 4, 834–994. doi:10.1016/B978-0-12-818655-8.00138-4

Turksoy, F., Wallis, J. D., Tunca, U., and Ozturk, T. (2003). An in-depth study of the formation of new tetrathiafulvalene derivatives from 1,8-diketones. *Tetrahedron* 59 (41), 8107–8116. doi:10.1016/j.tet.2003.08.042

Wang, J., Liu, K., Ma, L., and Zhan, X. (2016). Triarylamine: Versatile platform for organic, dye-sensitized, and perovskite solar cells. *Chem. Rev.* 116, 14675–14725. doi:10.1021/acs.chemrev.6b00432

Wolff, C. M., Bourelle, S. A., Phuong, L. Q., Kurpiers, J., Feldmann, S., Capriolgio, P., et al. (2021). Orders of recombination in complete perovskite solar cells – linking time-resolved and steady-state measurements. *Adv. Energy Mat.* 11, 2101823. doi.org/doi:10.1002/aenm.202101823

Wu, Y., Wang, Z., Liang, M., Cheng, H., Li, M., Liu, L., et al. (2018). Influence of nonfused cores on the photovoltaic performance of linear triphenylamine-based hole-transporting materials for perovskite solar cells. *ACS Appl. Mat. Interfaces* 10 (21), 17883–17895. doi:10.1021/acsami.8b02090

Xu, Y., Huang, F., and Li, W. (2020). Schottky-Barrier-Dependent electrical characteristics in conjugated polymer transistors with various contact metals. *Front. Mat.* 7, 131. doi:10.3389/fmats.2020.00131

Yildiz, G., Aydogmus, Z., Cinar, M. E., Senkal, F., and Ozturk, T. (2017). Electrochemical oxidation mechanism of eugenol on graphene modified carbon paste electrode and its analytical application to pharmaceutical analysis. *Talanta* 173, 1–8. doi:10.1016/j.talanta.2017.05.056

Zhang, F., Wang, Z., Zhu, H., Pellet, N., Luo, J., Yi, C., et al. (2017). Over 20% PCE perovskite solar cells with superior stability achieved by novel and low-cost hole-transporting materials. *Nano Energy* 41, 469–475. doi:10.1016/j.nanoen.2017.09.035